

Study on Temperature-Dependent Changes in Hydrogen Bonds in Cellulose I β by Infrared Spectroscopy with Perturbation-Correlation Moving-Window Two-Dimensional Correlation Spectroscopy

Akihiko Watanabe,^{†‡} Shigeaki Morita,[†] and Yukihiko Ozaki^{*,†}

Department of Chemistry and Research Center for Near Infrared Spectroscopy, School of Science and Technology, Kwansai Gakuin University, 2-1 Gakuen, Sanda 669-1337, Japan, and R&D Unit, Yasuma Co. Ltd., 2100 Nakagawa, Morimachi, Shuchi-gun 437-0223, Japan

Received April 14, 2006; Revised Manuscript Received September 9, 2006

Infrared (IR) spectra were measured for cellulose I β prepared from the mantle of *Halocynthia roretzi* over a temperature range of 30–260 °C to explore the temperature-dependent changes in hydrogen bonds (H-bonds) in the crystal. Structural changes at the phase transition temperature of 220 °C are elucidated at the functional group level by perturbation-correlation moving-window two-dimensional (PCMW2D) correlation spectroscopy. The PCMW2D correlation spectra show that the intensities of bands arising from O3–H3···O5 and O2–H2···O6 intrachain H-bonds dramatically decrease at 220 °C, whereas the intensity changes of bands due to interchain H-bonds are not observed adequately. These results suggest that the phase transition is induced by the dissociation of the O3–H3···O5 and O2–H2···O6 intrachain H-bonds. However, the interchain H-bonds are not so much responsible for the transition directly.

Introduction

Cellulose, 1,4- β -glucan, is often said to be the most abundant polymer on the earth.^{1–3} It is certainly one of the most important structural elements in plants and other living systems.^{1–3} Figure 1 illustrates a structure of cellulose. Native cellulose such as wood and cotton cellulose contains cellulose I structure.^{1–4} According to the literature,^{1–6,11–14} there are inter- and intrachain H-bonds in cellulose I; a secondary OH group at the C3 position forms a H-bond with an O5 atom of the adjacent ring (O3–H3···O5 intrachain H-bond), and another secondary OH group at the C2 position constructs a H-bond with an O6 atom of the adjacent ring (O2–H2···O6 intrachain H-bond). A primary OH group at the C6 position constitutes a H-bond with an O3 atom in the neighboring chain (O6–H6···O3' interchain H-bond). These H-bonds are considered to be responsible for various properties of native cellulose such as single-chain conformation, stiffness, and solubility in solvent.^{1–3,7–10}

Infrared spectroscopy is sensitive to the conformation and local molecular environment of molecules including biopolymers.^{15,16} An IR spectrum of cellulose contains much information about the inter- and intrachain H-bonds.^{14,17–26} Therefore, it has been employed to elucidate the structure of cellulose.^{14,17–26} Our research group recently investigated temperature-dependent structural changes in H-bonds in cotton cellulose¹⁹ and microcrystalline cellulose (MCC)²⁰ by using IR spectroscopy. From the former study,¹⁹ it was indicated that a structural change of the less stable I α phase occurs in the temperature range of 40–150 °C, whereas the breakings of intrachain H-bonds take place in the temperature range of 250–320 °C. The latter study suggested that a glass transition of MCC at 184 °C induces

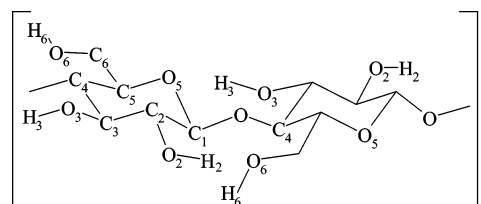


Figure 1. Structure of cellulose.

drastic structural changes in the H-bond network of MCC.²⁰ It is well-known that cellulose I exists in two crystalline forms, i.e., I α and I β .^{1–3} However, the information about respective thermal behavior of H-bonds in I α and I β phases could not be obtained adequately from these studies. There has been a number of studies exploring the thermal behavior of I α phase because a transformation from unstable I α phase to stable I β phase in heat treatment is one of the most striking phenomena of native cellulose.^{3,22,27–31} Although cellulose I β abundantly exists in the cell walls of a wide range of higher plants such as wood and cotton,^{1,3} there has been only a few reports describing thermal behavior of neat cellulose I β .^{14,32} On the basis of an X-ray diffraction study, Wada³² showed that cellulose I β prepared from the mantle of tunicate transforms into the high-temperature phase with a temperature increase above 220–230 °C. However, a process of the transition has not been elucidated at the functional group level sufficiently.

In the present study, tunicate cellulose, which is considered as a standard material for cellulose I β ^{12,22,32} is used for measuring temperature-dependent IR spectra in order to obtain exclusively information about the thermal behavior of cellulose I β at the functional group level. However, it is not straightforward to interpret spectral variations in the IR spectra because bands due to the OH groups of cellulose are heavily overlapped in the O–H stretching vibration region. Therefore, one must look for a powerful tool that enables the unraveling of the overlapping bands.

* To whom correspondence should be addressed. Fax: +81-79-565-9077. E-mail: ozaki@kwansai.ac.jp.

[†] Kwansai Gakuin University.

[‡] Yasuma Co. Ltd.

Our research group (Morita et al.) has recently proposed perturbation-correlation moving-window two-dimensional (PCMW2D) correlation spectroscopy.³³ This new spectra analysis method was developed from generalized 2D correlation spectroscopy (2DCOS) proposed by Noda in 1993^{34–36} and moving-window 2D (MW2D) correlation spectroscopy by Thomas and Richardson in 2000.³⁷ The PCMW2D correlation analysis provides a pair of synchronous and asynchronous 2D correlation spectra plotted on a plane between spectral variable (e.g., wavenumber) axis and a perturbation variable (e.g., temperature) axis. One of the advantages of the PCMW2D correlation analysis is that it can clearly point out both a specific perturbation (e.g., melting temperature) and a characteristic spectral variable (e.g., corresponding band position) from spectral variations induced by a perturbation, even if it is applied for complicated spectra such as spectra that band positions cannot be identified in raw spectra; furthermore, the positions show shift with the perturbation.^{33,38} By interpreting the PCMW2D correlation spectra, a pattern of structural changes (e.g., gradual and rapid) in an object in all perturbation ranges can be elucidated. In our previous study,²⁰ the PCMW2D correlation analysis extracted useful information about the structural change of MCC from the complicated temperature-dependent IR and near-infrared (NIR) spectra (25–200 °C). It was suggested from the study that the disruptions of the O–H···O(H) H-bonds in MCC gradually occur in the temperature range of 25–130 °C, whereas they become greater above 130 °C and attain a maximum at the glass transition temperature of 184 °C. Thus, it is expected that the PCMW2D correlation analysis divides the heating process of cellulose I β into some stages and makes it possible to clarify the structural changes in the respective stages.

The purpose of the present study is to investigate the thermal behavior of cellulose I β by using temperature-dependent IR spectra in the O–H stretching and C–O stretching of H-bonds sensitive bands regions. PCMW2D correlation spectroscopy was utilized for the interpretation of the spectra. A phase transition of cellulose I β around 220 °C, which was proposed by Wada,³² and a process before the transition (30–220 °C) have been elucidated at the functional group level.

Experimental Section

Preparation of a Cellulose Film.^{22,30–32} Tunicate cellulose, which had high crystallinity and consisted almost completely of pure I β cellulose,^{12,22,32} was used in this study. The tunicate cellulose was extracted from the mantle of *Halocynthia roretzi* harvested in the offing of Sanriku, Japan. It was purified by immersion in a 5% KOH aqueous solution for 12 h at room temperature and then treated with a 0.3% NaClO₂ aqueous solution buffered at pH 4.9 with acetate buffer at 70 °C for 3 h. These procedures were repeated until the mantle became completely white. The purified sample was disintegrated into small fragments using a homogenizer. After homogenization, it was hydrolyzed by treating with 50% sulfuric acid at 50 °C for 8 h under continuous stirring in order to make a suspension of cellulose microcrystal. The solid content of the sample after hydrolysis was collected by centrifugation (at 600g), and then it was diluted with deionized water. These procedures are repeated until the supernatant in the tube became turbid (This turbid supernatant contains microcrystal of cellulose I β). The turbid supernatant was collected and then neutralized by a 5% NaOH aqueous solution (cellulose suspension). A few drops of the cellulose suspension was put onto a CaF₂ plate and then dried at 40 °C. A film of cellulose I β prepared on the CaF₂ plate was washed by deionized water and then dried at room temperature until the peak in the 1700–1600 cm⁻¹ region assigned to the water

O–H deformation band completely disappeared. All peak positions in an IR spectrum of the cellulose film (in the regions of 3600–2800 and 1500–1000 cm⁻¹) almost completely corresponded to those of the literature.¹⁴

Methods. The cellulose film prepared on a CaF₂ plate was put into a homemade cell for transmittance IR measurement equipped with a temperature controller. The temperature-dependent IR spectra were measured under the purge of dried nitrogen gas. All of the IR spectra were obtained at a resolution of 2 cm⁻¹ with a NEXUS 870 FT-IR spectrometer (Thermo Nicolet) equipped with a deuterated triglycine sulfate (DTGS) detector, and 128 scans were coadded for each spectrum. A series of transmission IR spectra was collected from 30 to 260 °C at every 1 °C increments in a rate of ca. 0.2 °C/min; that is, 231 spectra were obtained. All of the IR spectra are given in an absorbance unit defined as $-\log(I/I_0)$, where I and I_0 are the intensities of signals from the sample on the CaF₂ plate at respective temperature and the CaF₂ plate without the sample at 30 °C, respectively. Second derivative spectra were calculated by the Savitzky-Golay method³⁹ using homemade software. Before second derivative and PCMW2D analysis, all of the obtained spectra were subjected to Kawata-Minami smoothing⁴⁰ by using homemade software for spectral noise reduction.

Perturbation-Correlation Moving-Window Two-Dimensional Correlation Spectroscopy. Mathematical procedure and numerical computation of the PCMW2D correlation spectroscopy have been described in detail elsewhere.³³ A basic concept of PCMW2D correlation spectroscopy is described below. At first, consider a spectral intensity data matrix $y(v,p)$ consisting of rows along the spectral variable and columns along the perturbation variable, where v and p are wavenumber and perturbation of temperature, respectively. PCMW2D correlation spectroscopy uses a small window of a sub-divided data matrix with a window size of $2m + 1$ as

$$y_j(v,p_j) = \begin{pmatrix} y(v,p_{j-m}) \\ y(v,p_{j-m+1}) \\ \vdots \\ y(v,p_j) \\ \vdots \\ y(v,p_{j+m}) \end{pmatrix} \quad (1)$$

The sub-divided matrix is prepared by picking up a series of J th spectrum by incrementing J from $j - m$ to $j + m$. Note that j and J correspond respectively to the index of a window and the index of a spectrum within the window. Synchronous and asynchronous PCMW2D correlation spectra are calculated as follows:

$$\Pi_{\Phi,j}(v,p_j) = \frac{1}{2m} \sum_{J=j-m}^{j+m} \tilde{y}(v,p_J) \cdot \tilde{p}_J \quad (2)$$

$$\Pi_{\Psi,j}(v,p_j) = \frac{1}{2m} \sum_{J=j-m}^{j+m} \tilde{y}(v,p_J) \cdot \sum_{K=j-m}^{j+m} M_{JK} \cdot \tilde{p}_K \quad (3)$$

where $\tilde{y}(v,p_j)$ and \tilde{p}_j are dynamic spectrum and dynamic perturbation in the j th window, respectively.³³ M_{JK} is the element of discrete Hilbert–Noda transformation matrix.³⁶

The PCMW2D correlation spectra are obtained by incrementally sliding the window position from $j = 1 + m$ to $j = N - m$ (N is the total number of spectra) and calculating eqs 2 and 3 for each window. According to the study by Morita et al.,³³ the synchronous and asynchronous PCMW2D correlation spectra are proportional to first perturbation derivative and opposite sign of perturbation second derivative, respectively

$$\Pi_{\Phi}(v,p) \sim \left(\frac{\partial y(v,p)}{\partial p} \right)_v \quad (4)$$

$$\Pi_{\Psi}(v,p) \sim -\left(\frac{\partial^2 y(v,p)}{\partial p^2}\right)_v \quad (5)$$

Spectral variations can be interpreted by the combination of synchronous and asynchronous PCMW2D correlation spectra with the aid of the rules of the PCMW2D correlation spectroscopy for the case of linear increment perturbation proposed by Morita et al.³³ The rules are summarized in Table 1.³³ In the present study, all of the PCMW2D correlation spectra were calculated by homemade software named "2Dshige" (<http://sci-tech.ksc.kwansei.ac.jp/~ozaki/>).³³

Results and Discussion

IR Spectra in the O–H Stretching Region. Figure 2a shows temperature-dependent IR spectra in the 3600–3100 cm⁻¹ region of cellulose I β (30–260 °C). These spectra were collected with a 1 °C increment (total 231 spectra, only 17 spectra are shown here). Bands observed in this region are assigned to the stretching modes of OH groups of cellulose.^{4,14,17,19–26} Peaks at 3340 and 3276 cm⁻¹ are identified in the spectrum (at 30 °C). It can be seen from the figure that the intensities of these peaks decrease and the peaks shift to a higher wavenumber with temperature. These observations reveal that the structure of cellulose I β changes with temperature.

Second derivative spectra of the temperature-dependent IR spectra (3600–3100 cm⁻¹) are shown in Figure 2b. At least six peaks are identified in the second derivative spectra. Maréchal and Chanzy¹⁴ have proposed detailed assignments for IR bands in the O–H stretching and C–O stretching regions of cellulose I β prepared from hydrothermally treated Valonia microcrystal by using polarized IR spectra. In the present study, the band assignments in the O–H stretching and C–O stretching regions are mainly based on their assignments. Peaks at 3339 and 3270 cm⁻¹ (at 30 °C) are attributed to the O3–H3···O5 intrachain H-bonds and the O2–H2···O6 intrachain H-bonds, respectively. Liang and Marchessault¹⁷ have also assigned the band at 3350 cm⁻¹ to the O3–H3···O5 intrachain H-bonds. Features at 3413 and 3301 cm⁻¹ (at 30 °C) arise from the primary OH groups forming O6–H6···O3' interchain H-bonds.¹⁴ The interchain H-bonds are almost perpendicularly constructed to the cellulose chain.^{1–6,11–14} From IR studies of cellulose I not only by Maréchal et al.¹⁴ but also by other researchers,^{17,23} it was shown that the transition dipole moments of the bands at 3413 and 3301 cm⁻¹ are perpendicular to the axis of the cellulose chain, indicating that these bands are due to the OH groups forming the interchain H-bonds. A peak at 3376 cm⁻¹ (at 30 °C) is also attributed to the primary OH groups with H-bond; however, the H-bond structure has not been clarified.¹⁴ The weak peak near 3470 cm⁻¹ that appeared above 170 °C is assigned to the OH groups with weak H-bonds (this H-bond structure has also not been revealed).¹⁴

Table 1. Rules of PCMW2D Correlation Spectroscopy (in the Case of Linear Increment Perturbation)³³

Synchronous	Asynchronous	Spectral change	
+	+	Convex increment	↗
+	0	Linear increment	↘
+	-	Concave increment	↖
0	0	Constant	→
-	+	Convex decrement	↘
-	0	Linear decrement	↗
-	-	Concave decrement	↖

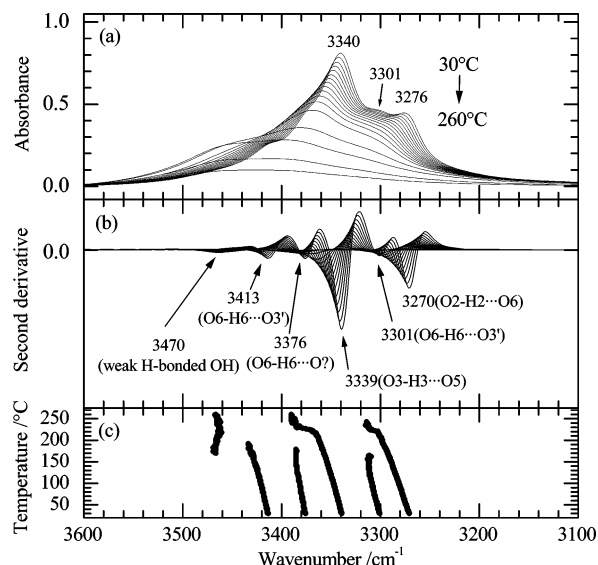


Figure 2. (a) Temperature-dependent IR spectra in the 3600–3100 cm⁻¹ region of cellulose I β (30–260 °C). Representative spectra are shown in the figure. (b) Second derivative spectra of the spectra shown in panel a. (c) Peak positions as a function of temperature determined by the local minimum of the second derivative spectra.

Figure 2c plots the peak positions as a function of temperature determined from local minima of the second derivative spectra. The peaks except for the peak near 3470 cm⁻¹ shift to a higher wavenumber with temperature. These shifts reflect that the inter- and intrachain H-bonds become weak with temperature. The shifts of the peaks at 3339 and 3270 cm⁻¹, which are assigned to the intrachain H-bonds, are gradual below 220 °C but become much faster above 220 °C. This result suggests that the structural changes in these intrachain H-bonds are gradual below 220 °C and that they suddenly become greater above 220 °C. The appearance of the weak peak near 3470 cm⁻¹ above 170 °C implies the formation of a structure with weak H-bonds above this temperature. The peaks at 3413 and 3301 cm⁻¹, attributed to the O6–H6···O3' interchain H-bonds, disappear above 200 °C. This observation indicates that the structural changes in the interchain H-bonds complete below 200 °C.

It has been clear from the raw spectra (Figure 2a) that increasing structure and decreasing structure exist during the heating process; the second derivative spectra cannot explain these changes sufficiently. In order to explore the structural changes in the H-bonds in cellulose I β in more detail, information about intensity changes in the raw spectra must be extracted more precisely. However, the spectra in the O–H stretching vibration region are broad, especially in the high-temperature range, and many OH bands due to the OH groups with different strength of H-bonds are heavily overlapping. Moreover, these OH bands shift with temperature. Therefore, it is not straightforward to obtain information about the structural changes in cellulose I β from the raw spectra directly. In the next subsection, spectral variations in the raw spectra have adequately been analyzed by the PCMW2D correlation spectroscopy.

PCMW2D Correlation Analysis in the O–H Stretching Region. Figure 3a shows a synchronous PCMW2D correlation spectrum constructed from the temperature-dependent IR spectra in the region of 3600–3100 cm⁻¹ of cellulose I β ($2m + 1 = 25$). Positive and negative correlation areas are represented by white and gray color, respectively. In the temperature range of 30–200 °C, two negative correlation valley bottoms are observed in the 3380–3320 and 3310–3240 cm⁻¹ regions. The bands presented in the 3380–3320 and 3310–3240 cm⁻¹

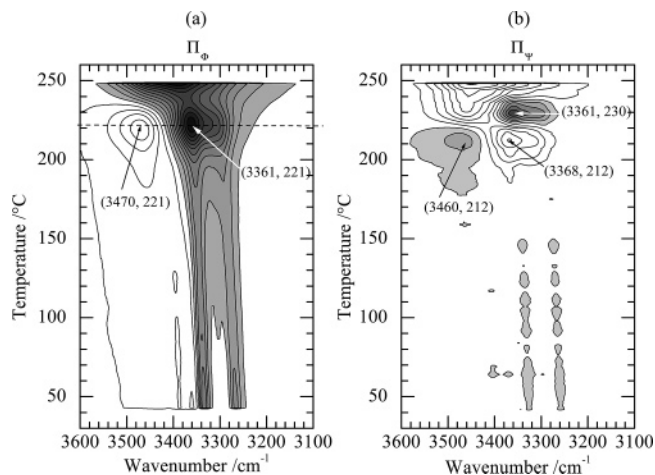


Figure 3. (a) Synchronous and (b) asynchronous PCMW2D correlation spectra in the 3600–3100 cm^{-1} region calculated from the temperature-dependent IR spectra of cellulose I β measured over a temperature range of 30–260 $^{\circ}\text{C}$.

regions are assigned to the O3–H3 \cdots O5 intrachain H-bonds and the O2–H2 \cdots O6 intrachain H-bonds, respectively (Figure 2b). When a band shows a negative correlation value in a synchronous PCMW2D correlation spectrum, the intensity of the band decreases with perturbation of temperature (see eq 4). Therefore, these negative correlation valley bottoms reveal that the intensities of the bands due to the O3–H3 \cdots O5 intrachain H-bonds and the O2–H2 \cdots O6 intrachain H-bonds decrease in the temperature range of 30–200 $^{\circ}\text{C}$; that is, the ruptures of these intrachain H-bonds mainly occur in this temperature range. These two negative correlation valley bottoms shift to a high wavenumber with temperature. This result reflects that the intrachain H-bonds are gradually weakened with temperature. A very low negative correlation valley bottom around 3300 cm^{-1} is observed in the temperature range of 90–150 $^{\circ}\text{C}$, indicating a structural change in the interchain H-bonds (Figure 2b). In the raw spectrum at 30 $^{\circ}\text{C}$, the intensities of the bands at 3301 and 3276 cm^{-1} are in the same level (Figure 2a), whereas the negative correlation intensity of the band at 3270 cm^{-1} is much larger than that of the band at 3301 cm^{-1} . Thus, the strength of the relative intensity of a band is not always correlated to that of the PCMW2D correlation intensity of the band. It is suggested that the structural change in the interchain H-bonds is smaller than that in the intrachain H-bonds.

Figure 3b shows an asynchronous PCMW2D correlation spectrum calculated from the temperature-dependent IR spectra of cellulose I β in the region of 3600–3100 cm^{-1} ($2m + 1 = 25$). In the temperature range of 30–200 $^{\circ}\text{C}$, the asynchronous correlation values of the bands in the 3380–3320 and 3310–3240 cm^{-1} regions show almost zero correlation intensities. An asynchronous PCMW2D correlation spectrum is proportional to the opposite sign of the second derivative of an intensity change with respect to temperature (see eq 5). Therefore, the decreases in the intensities of the bands in the 3380–3320 and 3310–3240 cm^{-1} regions are linear (see Table 1). It is revealed from the synchronous and asynchronous PCMW2D correlation spectra that the disruptions of the O3–H3 \cdots O5 intrachain H-bonds and the O2–H2 \cdots O6 intrachain H-bonds gradually happen in the temperature range of 30–200 $^{\circ}\text{C}$. It is also clarified from the synchronous PCMW2D correlation spectrum that the disruptions of these two types of intrachain H-bonds take place at the same time in the temperature range.

In the temperature range of 200–230 $^{\circ}\text{C}$, the intensity change of the band at 3361 cm^{-1} should be noteworthy. A minimum

correlation peak at Π_{Φ} (3361 cm^{-1} , 221 $^{\circ}\text{C}$) is identified in the synchronous PCMW2D correlation spectrum. Since a synchronous PCMW2D correlation spectrum is proportional to a spectral gradient along temperature (see eq 4), the negative correlation peak indicates that the slope of the decrease in the intensity of the band at 3361 cm^{-1} becomes the maximum at 221 $^{\circ}\text{C}$. In the asynchronous PCMW2D correlation spectrum, a positive correlation peak and a negative correlation peak are observed at Π_{Ψ} (3368 cm^{-1} , 212 $^{\circ}\text{C}$) and Π_{Ψ} (3361 cm^{-1} , 230 $^{\circ}\text{C}$), respectively. Based on the rules of PCMW2D correlation analysis (Table 1), since both the synchronous correlation values at Π_{Φ} (3368 cm^{-1} , 212 $^{\circ}\text{C}$) and Π_{Φ} (3361 cm^{-1} , 230 $^{\circ}\text{C}$) show negative, the former asynchronous correlation peak indicates that the intensity of the band at 3368 cm^{-1} convexly decreases at 212 $^{\circ}\text{C}$. On the other hand, the later one suggests that the intensity of the band at 3361 cm^{-1} concavely decreases at 230 $^{\circ}\text{C}$. The asynchronous correlation value at 3361 cm^{-1} changes from positive to negative in the temperature around 220 $^{\circ}\text{C}$. This result shows that the decrease in the intensity of the band at 3361 cm^{-1} becomes rapid around 220 $^{\circ}\text{C}$ from a convex decrease to a concave decrease. The band at 3361 cm^{-1} is assigned to the O3–H3 \cdots O5 intrachain H-bonds (see Figure 2). Therefore, these results elucidate that the O3–H3 \cdots O5 intrachain H-bonds are dramatically disrupted around 220 $^{\circ}\text{C}$.

In the synchronous PCMW2D correlation spectrum, a positive correlation peak at Π_{Φ} (3470 cm^{-1} , 221 $^{\circ}\text{C}$) is observed. The correlation peak reveals that the increase in the intensity of the band at 3470 cm^{-1} becomes the maximum at 221 $^{\circ}\text{C}$ (see eq 4). The band at 3470 cm^{-1} is assigned to the OH groups with weak H-bonds (see Figure 2). Although the H-bond structure cannot be clarified, the weak H-bonded OH groups probably appear in concert mainly with the structural changes in the intrachain H-bonds because Figure 3a indicates that the intensity of the band at 3470 cm^{-1} increases with the decreases in the bands of the intrachain H-bonds. In the asynchronous PCMW2D correlation spectrum, a negative correlation peak is located at Π_{Ψ} (3460 cm^{-1} , 212 $^{\circ}\text{C}$). Based on the rules of PCMW2D correlation analysis, since the synchronous correlation value at Π_{Φ} (3460 cm^{-1} , 212 $^{\circ}\text{C}$) is positive (Table 1), the intensity of the band at 3460 cm^{-1} concavely increases at 212 $^{\circ}\text{C}$. The asynchronous correlation values at 3470 cm^{-1} change from negative to positive (indicating convex increment) in the temperature around 220 $^{\circ}\text{C}$. This result shows that the increase in the intensity of the band at 3470 cm^{-1} becomes rapid around 220 $^{\circ}\text{C}$. These observations indicate that a structure with weak H-bonds is formed drastically around 220 $^{\circ}\text{C}$; a significant structural change in the cellulose I β emerges around this temperature. The intensity of the band in the C=O stretching region (1800–1700 cm^{-1}) increases above ca. 230 $^{\circ}\text{C}$, indicating the thermal degradation of cellulose (the result is not shown).²⁴ Broad negative correlation values observed in the synchronous PCMW 2D correlation spectrum above 240 $^{\circ}\text{C}$ are due to the thermal degradation of cellulose.

Figure 4 depicts a slice spectrum at 221 $^{\circ}\text{C}$ extracted from the synchronous PCMW2D correlation spectrum in Figure 3a. The slice point is given in Figure 3a by a dashed line. A negative peak identified at 3361 cm^{-1} is due to the O3–H3 \cdots O5 intrachain H-bonds. A negative shoulder is observed near 3300 cm^{-1} . The position of the shoulder corresponds to that of the second derivative peak attributed to the O2–H2 \cdots O6 intrachain H-bonds (221 $^{\circ}\text{C}$). Therefore, the shoulder indicates a structural change in the O2–H2 \cdots O6 intrachain H-bonds. The asynchronous correlation value near 3300 cm^{-1} also changes from positive to negative in the temperature around 220 $^{\circ}\text{C}$. From

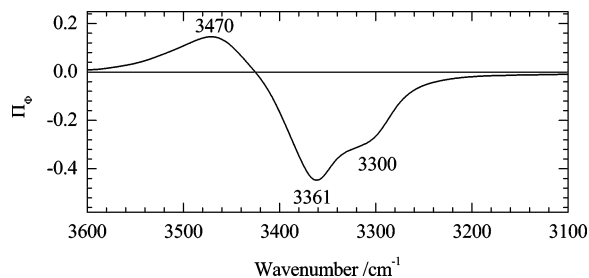


Figure 4. Slice spectrum extracted from the synchronous PCMW2D correlation spectrum in Figure 3a at 221 °C.

these observations, the O2–H2···O6 intrachain H-bonds as well as the O3–H3···O5 intrachain H-bonds are rapidly disrupted at 221 °C. The ratio of the negative correlation intensity at 3300 cm^{-1} (221 °C) to that at 3361 cm^{-1} (221 °C) is 0.59. The ratio of absorbance at 3276 (O2–H2···O6 intrachain H-bonds) to 3340 cm^{-1} (O3–H3···O5 intrachain H-bonds) in the raw spectrum at 30 °C (Figure 2a) is 0.55. These ratios are almost similar to each other. This result indicates that a proportion of the number of initial O3–H3···O5 intrachain H-bonds and the number of disruption of the H-bonds at 221 °C is almost the same as that of O2–H2···O6 intrachain H-bonds. Therefore, the ruptures of the O3–H3···O5 intrachain H-bonds and the O2–H2···O6 intrachain H-bonds gradually occur below 200 °C. They are accelerated above 200 °C, and then drastic disruptions of these intrachain H-bonds take place around 220 °C. The second derivative peaks at 3339 and 3270 cm^{-1} , which are assigned to the O3–H3···O5 intrachain H-bonds and the O2–H2···O6 intrachain H-bonds, respectively, rapidly shift to a higher wavenumber above 220 °C (Figure 2c). Therefore, the results of the PCMW2D correlation analysis are in good agreement with those of the second derivative analysis.

On the basis of an X-ray diffraction study of the heating process of cellulose I β , Wada³² showed that cellulose I β undergoes a transition into the high-temperature phase with the temperature increase above 220 °C. As described above, it has been revealed from the PCMW2D correlation analysis that the significant intensity changes of the bands at 3470, 3361, and 3300 cm^{-1} happen around 220 °C, indicating the decrease in the structure with strong H-bonds and the formation of the structure with weak H-bonds. The phase transition revealed by Wada is well reflected in the temperature-dependent IR spectra. In other words, our results support the existence of the “high-temperature structure of cellulose I” proposed by Wada.³² It should be noted that the transition is elucidated at the functional group level by the present study; the transition is mainly induced by the disruptions of the O3–H3···O5 and O2–H2···O6 intrachain H-bonds. Since the intensity changes of the bands due to the interchain H-bonds are not observed adequately around the temperature, it is likely that the interchain H-bonds are not much related to the phase transition directly. It seems that the structural changes in the interchain H-bonds complete below 200 °C because the second derivative peaks at 3413 and 3301 cm^{-1} (at 30 °C), which are assigned to the O6–H6···O3' interchain H-bonds, disappear above 200 °C (Figure 2c). In an IR study of cellulose I β by Maréchal et al.,¹⁴ a subtraction spectrum was obtained by subtracting the spectrum at 115 °C from the spectrum at 25 °C, and then two positive peaks at 3340 and 3267 cm^{-1} , indicating the structural changes of the intrachain H-bonds, were identified. However, they have not clarified the details of the process of the structural changes in the H-bonds in the temperature range of 25–115 °C and the structural changes above 115 °C. As mentioned above, not only

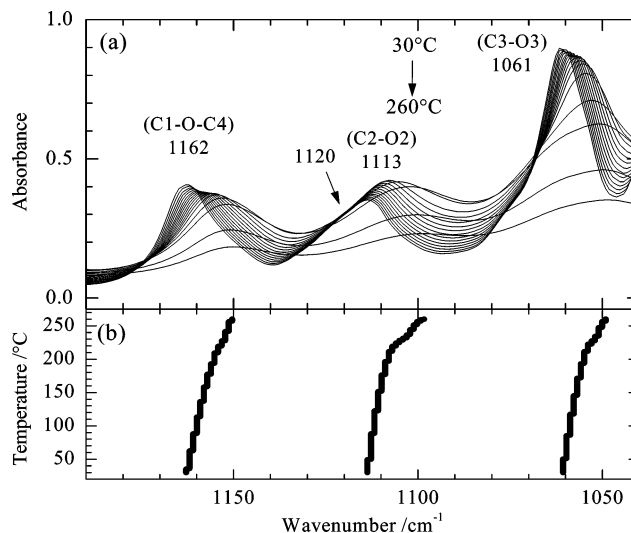


Figure 5. (a) Temperature-dependent IR spectra in the 1190–1040 cm^{-1} region of cellulose I β (30–260 °C). Representative spectra are shown in the figure. (b) Peak positions as a function of temperature determined by the local maximum of the spectra.

the process of the structural changes in the intrachain H-bonds in the temperature range of 25–115 °C but also the thermal behavior of cellulose I β above 115 °C are revealed by the present study. The PCMW2D correlation analysis can extract useful information about temperature-dependent changes in the OH···O(H) H-bonds in cellulose from complicated spectral variations in the O–H stretching region where many OH bands are heavily overlapping and show temperature-dependent shifts.

IR Spectra in the C–O Stretching Region. Figure 5a shows the temperature-dependent IR spectra in the 1190–1040 cm^{-1} region of cellulose I β measured over a temperature range of 30–260 °C. These spectra were collected with a 1 °C increment (total 231 spectra, only 17 spectra are shown here). A peak at 1162 cm^{-1} is observed in the IR spectrum at 30 °C. According to the literature,^{14,18} the transition dipole moment of the band at 1162 cm^{-1} is entirely parallel to the axis of the cellulose chain; therefore, it has been assigned to the antisymmetric C–O–C stretching mode of β 1,4-glycosidic bonds. Based on an IR study by Maréchal et al.,¹⁴ peaks at 1113 and 1061 cm^{-1} at 30 °C arise from the C–O stretching modes of C2–O2 and C3–O3 groups, respectively. They¹⁴ revealed by using the polarized spectra that the peak at 1115 cm^{-1} observed in a raw spectrum of cellulose I β is overlapped by two features at 1121 and 1112 cm^{-1} , implying the existence of same alcohol with different H-bonds (also in Figure 5a, a shoulder near 1120 cm^{-1} is observed). In their study,¹⁴ it was suggested that there are O2–H2 groups with different H-bond structures in cellulose I β ; one is involved in a strong O2–H2···O6 intrachain H-bond, and the others are involved in weak or no H-bonds (the structures are not elucidated). They confirmed that the intensity of the band at 1121 cm^{-1} decreases by heating at 115 °C, whereas the intensity of the band at 1112 cm^{-1} increases. From these observations, they assigned the bands at 1121 and 1112 cm^{-1} to the C2–O2 groups with the O2–H2···O6 intrachain H-bonds and those with weak or no H-bond, respectively. In the same study,¹⁴ they also clarified that both the lower wavenumber shift of the peak at 1060 cm^{-1} by heating at 115 °C and that by evaporation of D₂O molecules after the H/D exchange are correlated to the intensity change of the band due to the O3–H3 groups and assigned the band at 1060 cm^{-1} to the C3–O3 groups.

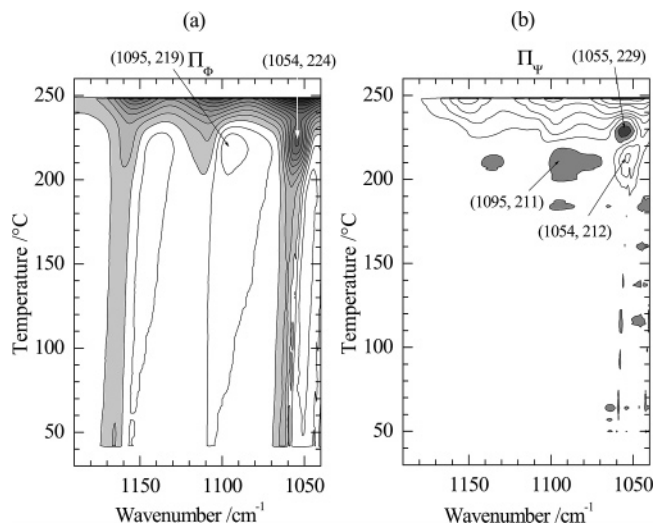


Figure 6. (a) Synchronous and (b) asynchronous PCMW2D correlation spectra in the 1190–1040 cm^{-1} region calculated from the temperature-dependent IR spectra of cellulose I β collected over a temperature range of 30–260 $^{\circ}\text{C}$.

Figure 5b plots the peak positions as a function of temperature determined from the local maxima of the temperature-dependent IR spectra. All of the peaks shift to a lower wavenumber with temperature. The shifts of the peaks at 1113 and 1061 cm^{-1} are gradual in the temperature range of 30–220 $^{\circ}\text{C}$, whereas the shifts of these peaks become larger above 220 $^{\circ}\text{C}$. In the previous section, it has been revealed that the rapid intensity changes of the bands due to the intrachain H-bonds at 221 $^{\circ}\text{C}$ are related to the phase transition.³² Therefore, it is likely that the drastic shifts of the peaks at 1113 and 1061 cm^{-1} above 220 $^{\circ}\text{C}$ are also caused by the transition. The shift of the peak at 1162 cm^{-1} is almost constant. The shift of the peak at 1162 cm^{-1} above 220 $^{\circ}\text{C}$ is smaller than the shifts of the peaks at 1113 and 1061 cm^{-1} . It seems that the structural change in the β 1,4-glycosidic bonds above 220 $^{\circ}\text{C}$ is smaller than structural changes in the C2–O2 and C3–O3 groups.

PCMW2D Correlation Analysis in the C–O Stretching Region. A synchronous PCMW2D correlation spectrum constructed from the temperature-dependent IR spectra in the region of 1190–1040 cm^{-1} ($2m + 1 = 25$) of cellulose I β is shown in Figure 6a. A negative correlation peak is identified at Π_{Φ} (1054 cm^{-1} , 224 $^{\circ}\text{C}$) in the synchronous PCMW2D correlation spectrum. This peak indicates that the decrease in the intensity of the band at 1054 cm^{-1} , assigned to the C3–O3 group, becomes the maximum at 224 $^{\circ}\text{C}$. A broad positive correlation peak at Π_{Φ} (1095 cm^{-1} , 219 $^{\circ}\text{C}$) identified in the synchronous PCMW2D correlation spectrum reflects that the increases in the intensity of the band at 1095 cm^{-1} , attributed to the C2–O2 group, becomes the maximum at 219 $^{\circ}\text{C}$. These correlation peaks elucidate that the slopes of the structural changes of the C3–O3 and C2–O2 groups show the maximum around the transition temperature of 220 $^{\circ}\text{C}$. It should be noted that although the shift of the peak at 1061 cm^{-1} above 220 $^{\circ}\text{C}$ is not so strong (Figure 5b), the PCMW2D correlation spectra clearly show that the significant structural change in the C3–O3 group occurs at the temperature.

Figure 6b shows an asynchronous PCMW2D correlation spectrum calculated from the temperature-dependent IR spectra in the region of 1190–1040 cm^{-1} ($2m + 1 = 25$) of cellulose I β . In the asynchronous PCMW2D correlation spectrum, a positive correlation peak and a negative correlation peak are located at Π_{Ψ} (1054 cm^{-1} , 212 $^{\circ}\text{C}$) and Π_{Ψ} (1055 cm^{-1} , 229

$^{\circ}\text{C}$), respectively. According to the rules of PCMW2D correlation analysis, the intensity of the band at 1054 cm^{-1} convexly decreases at 212 $^{\circ}\text{C}$ and the intensity of the band at 1055 cm^{-1} concavely decreases at 229 $^{\circ}\text{C}$. This result elucidates that the intensity of the C3–O3 band (at 1054 cm^{-1}) drastically decreases around 220 $^{\circ}\text{C}$. The asynchronous correlation value of the band at 1095 cm^{-1} changes from negative to positive around 220 $^{\circ}\text{C}$. This observation reveals that the intensity of the C2–O2 band (at 1095 cm^{-1}) rapidly increases around 220 $^{\circ}\text{C}$. Thus, from the result of the PCMW2D correlation analysis in the C–O stretching region as well as from that in the O–H stretching region, it is shown that the structural changes in the C3–O3–H3 and C2–O2–H2 drastically take place around 220 $^{\circ}\text{C}$ and that they induce the phase transition of cellulose I β .

A negative correlation valley bottom with a lower wavenumber shift starting from 1165 cm^{-1} (at 42 $^{\circ}\text{C}$) and positive correlation peak top with a lower wavenumber shift starting from 1157 cm^{-1} at 42 $^{\circ}\text{C}$ are observed in the synchronous PCMW2D correlation spectrum. According to the calculation of the strain energy distribution of cellulose I by Tashiro et al.,⁹ the intrachain H-bonds suppress torsional deformation of the flexible β 1,4-glycosidic bonds. In the previous section, it has been revealed that the intrachain H-bonds are disrupted with temperature. Therefore, it is likely that the intensity changes in the 1070–1125 cm^{-1} region and the lower wavenumber shift of the peak at 1162 cm^{-1} (Figure 5b) reflect the increase in the flexibility of the β 1,4-glycosidic bonds with temperature. It may be concluded that two events are in progress in the heating process. At first, the disruptions of the O3–H3 \cdots O5 intrachain H-bonds and the O2–H2 \cdots O6 intrachain H-bonds make the β 1,4-glycosidic bonds flexible in the temperature range of 30–200 $^{\circ}\text{C}$. These structural changes gradually occur. Consequently, the increase in the flexibility of the β 1,4-glycosidic bonds induces the increase in the flexibility of the cellulose chain. As a result, this change leads to further disruptions of the intrachain H-bonds at the phase transition temperature of 220 $^{\circ}\text{C}$. Thus, it is suggested from the present study that the flexibility of the β 1,4-glycosidic bonds gradually increases with the ruptures of the intrachain H-bonds in the temperature range of 30–220 $^{\circ}\text{C}$, and it is also responsible for the transition.

Conclusion

The present study has aimed at exploring the thermal behavior of cellulose I β by using temperature-dependent IR spectra with PCMW2D correlation. Recently, on the basis of the X-ray diffraction study, Wada³² showed that the phase transition of cellulose I β happens above 220–230 $^{\circ}\text{C}$. In the present study, structural changes at the phase transition of cellulose I β around 220 $^{\circ}\text{C}$ and the process before the transition are elucidated at the functional group level by PCMW2D correlation analysis. The conclusions reached by the present study concerning the thermal behavior of cellulose I β (30–260 $^{\circ}\text{C}$) are described as follows.

(1) In the temperature range of 30–200 $^{\circ}\text{C}$, the disruptions of the O3–H3 \cdots O5 intrachain H-bonds and the O2–H2 \cdots O6 intrachain H-bonds mainly occur. The structural changes in these intrachain H-bonds gradually take place.

(2) Drastic collapses of these intrachain H-bonds and rapid formation of new structure with weak H-bonds happen around 220 $^{\circ}\text{C}$. These structural changes lead to the phase transition. The ratio of disruption of the O3–H3 \cdots O5 intrachain H-bonds and the O2–H2 \cdots O6 intrachain H-bonds at the transition

temperature is almost the same as the ratio of amount of the O3–H3···O5 intrachain H-bonds and that of the O2–H2···O6 intrachain H-bonds at 30 °C (i.e., the ratio of the initial amount of these H-bonds). Therefore, ruptures of both intrachain H-bonds are key factors for the transition. However, the O6–H6···O3' interchain H-bonds are not so much correlated to the transition; it seems that the structural changes in the interchain H-bonds complete below 200 °C.

(3) The fact that the disruption of the intrachain H-bonds makes the β 1,4-glycosidic bonds flexible has been indicated by the calculation of the strain energy distribution of cellulose I by Tashiro et al.⁹ From the present study, it is suggested that the gradual increase in the flexibility of the β 1,4-glycosidic bonds with the disruptions of the intrachain H-bonds in the temperature range of 30–220 °C is also an important factor for the phase transition.

The results obtained from the present study support the existence of the “high temperature form” of cellulose I reported by Wada.³²

Acknowledgment. This study was supported by the “Open Research Center” project (Research Center for Near Infrared Spectroscopy) for private universities: matching fund subsidy from MEXT (Ministry of Education, Culture, Sport, Science and Technology), 2001–2008. This study was also supported by Kwansai Gakuin University “Special Research” project (Research Center for Environment Friendly Polymers), 2004–2008. The authors thank Ms. Mika Matsubara (Yasuma Co. Ltd.) for the preparation of cellulose I β .

References and Notes

- (1) Klemm, D.; Schmauder, Hans-Perter; Heinze, T. In *Biopolymers, Polysaccharides II*; Baets, S. De., Vandamme, E. J., Steinbüchel, A., Eds.; Wiley-VCH: Weinheim, Germany, 2002; Volume 6.
- (2) Klemm, D.; Philipp, B.; Heinze, T.; Heinze, U.; Wagenknecht, W. *Comprehensive Cellulose Chemistry*; Wiley-VCH: Weinheim, Germany, 1998; Volume 1.
- (3) Pérez, S.; Mazeau, K. In *Polysaccharides, Structure and Functional Versatility*, 2nd ed.; Dumitriu, S., Eds.; Marcel Dekker: New York, 2005; pp. 41–68.
- (4) Kondo, T. In *Polysaccharides, Structure and Functional Versatility*, 2nd ed.; Dumitriu, S., Eds.; Marcel Dekker: New York, 2005; pp. 69–98.
- (5) Gardner, K. H.; Blackwell, J. *Biochim. Biophys. Acta* **1974**, *343*, 232.
- (6) Gardner, K. H.; Blackwell, J. *Biopolymers* **1974**, *13*, 1975.
- (7) Tashiro, K.; Kobayashi, M. *Polym. Bull.* **1985**, *14*, 213.
- (8) Kroon-Batenburg, L. M.; Kroon, J.; Northolt, M. G. *Polym. Commun.* **1986**, *27*, 290.
- (9) Tashiro, K.; Kobayashi, M. *Polymer* **1991**, *32*, 1516.
- (10) Kamide, K.; Okajima, K.; Kowsaka, K. *Polym. J.* **1992**, *24*, 71.
- (11) Heiner, A. P.; Sugiyama, J.; Teleman, O. *Carbohydr. Res.* **1995**, *273*, 207.
- (12) Nishiyama, Y.; Langan, P.; Chanzy, H. *J. Am. Chem. Soc.* **2002**, *124*, 9074.
- (13) Nishiyama, Y.; Sugiyama, J.; Chanzy, H.; Langan, P. *J. Am. Chem. Soc.* **2003**, *125*, 14300.
- (14) Maréchal, Y.; Chanzy, H. *J. Mol. Struct.* **2000**, *523*, 183.
- (15) Koenig, J. L. In *Specific Interaction and the Miscibility of Polymer Blends*; Coleman, M. M., Graf, J. F., Painter, P. C., Eds.; Technomic Publishing Co., Inc.: Basel, 1991; pp. 221–307.
- (16) Maumann, D. In *Infrared and Raman Spectroscopy of Biological Materials*; Gremlich, H.-U., Yan, B., Eds.; Marcel Dekker: Inc.: New York, 2001; pp. 323–377.
- (17) Liang, C. Y.; Marchessault, R. H. *J. Polym. Sci.* **1959**, *37*, 385.
- (18) Liang, C. Y.; Marchessault, R. H. *J. Polym. Sci.* **1959**, *39*, 269.
- (19) Kokot, S.; Czarnik-Matusewicz, B.; Ozaki, Y. *Biopolymers* **2002**, *67*, 456.
- (20) Watanabe, A.; Morita, S.; Ozaki, Y. *Appl. Spectrosc.* **2006**, *60*, 611.
- (21) Watanabe, A.; Morita, S.; Kokot, S.; Matsubara, M.; Fukai, K.; Ozaki, Y. *J. Mol. Struct.* in press.
- (22) Sugiyama, J.; Persson, J.; Chanzy, H. *Macromolecules* **1991**, *24*, 2461.
- (23) Blackwell, J.; Vasko, P. D.; Koernig, J. L. *J. Appl. Phys.* **1970**, *41*, 4375.
- (24) Łojewska, J.; Miśkowiec, P.; Łojewski, T.; Proniewicz, L. M. *Polym. Degrad. Stab.* **2005**, *88*, 512.
- (25) Michell, A. J. *Carbohydrate* **1990**, *197*, 53.
- (26) Michell, A. J. *Carbohydrate* **1993**, *241*, 47.
- (27) Horii, F.; Yamamoto, H.; Kitamaru, R.; Tanahashi, M.; Higuchi, T. *Macromolecules* **1987**, *20*, 2946.
- (28) Yamamoto, H.; Horii, F. *Macromolecules* **1993**, *26*, 1313.
- (29) Debzi, E. M.; Chanzy, H.; Sugiyama, J.; Tekely, P.; Excoffier, G. *Macromolecules* **1991**, *24*, 6816.
- (30) Imai, T.; Sugiyama, J. *Macromolecules* **1998**, *31*, 6275.
- (31) Wada, M.; Kondo, T.; Okano, T. *Polym. J.* **2003**, *35*, 155.
- (32) Wada, M. *J. Polym. Sci. Part B: Polym. Phys.* **2002**, *40*, 1095.
- (33) Morita, S.; Shinzawa, H.; Noda, I.; Ozaki, Y. *Appl. Spectrosc.* **2006**, *60*, 398.
- (34) Noda, I. *Appl. Spectrosc.* **1993**, *47*, 1329.
- (35) Noda, I.; Dowrey, A. E.; Marcott, C.; Story, G. M.; Ozaki, Y. *Appl. Spectrosc.* **2000**, *54*, 236A.
- (36) Noda, I. *Appl. Spectrosc.* **2000**, *54*, 994.
- (37) Thomas, M.; Richardson, H. H. *Vib. Spectrosc.* **2000**, *24*, 137.
- (38) Morita, S.; Shinzawa, H.; Noda, I.; Ozaki, Y. *J. Mol. Struct.*, in press.
- (39) Savitzky, A.; Golay, M. J. E. *Anal. Chem.* **1964**, *36*, 1627.
- (40) Kawata, S.; Minami, S. *Appl. Spectrosc.* **1984**, *38*, 49.

BM0603591